Small angle x-ray scattering to characterize charged soft matter

Matthew Tirrell
Institute for Molecular Engineering
University of Chicago
Argonne National Laboratory

mtirrell@uchicago.edu, @UChicagoIME

http://ime.uchicago.edu/

in collaboration with: Daniel V. Krogstad, Robert Farina and (the late) Edward J. Kramer, University of California, Santa Barbara; Samanvaya Srivastava, Jing Yu, Jun Mao and Wei Chen, Argonne National Laboratory

SRI Satellite Workshop Argonne National Laboratory: July 13-14, 2015
Emerging Opportunities in High Energy X-ray Science: The Diffraction Limited Storage Ring Frontier

Mono-valent salt concentration dependence of force curves

Surface Forces Apparatus:

Balastre, Li, Tirrell

Macromolecules 2002, *35*, 9480–9486

Force curve depending on [$NaNO_3$]

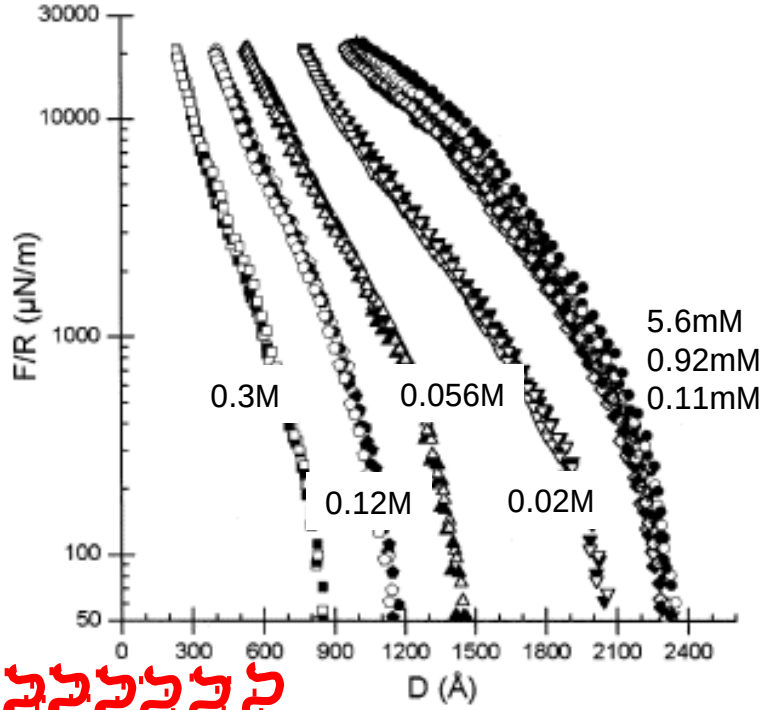

maximum brush height vs. [$NaNO_3$]

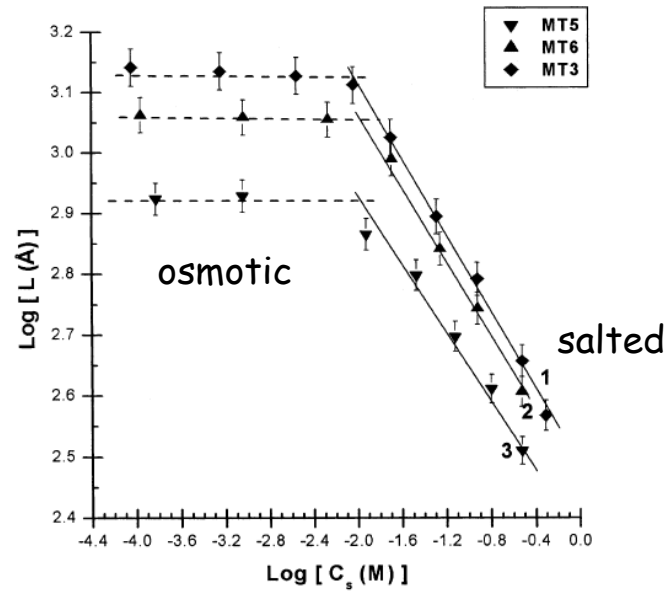

Figure 5. Salt concentration dependence of the brush height for the three different brushes. The solid and dashed lines are linear fits. The dashed lines have slopes close to zero. The slopes for the linear fit 1, 2, and 3 are −0.33 ± 0.02, −0.33 ± 0.02, and −0.30 ± 0.02, respectively.

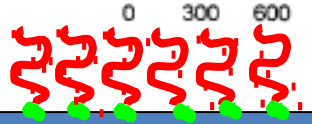

PSS brush w/small hydrophobic block

Elastic force Osmotic pressure L_0 = brush height

Osmotic brush regime

$$F \simeq \frac{3LkT}{Na^2} - \frac{\alpha NkT}{L} \longrightarrow L_0 \simeq \alpha^{1/2} Na$$

Pincus, 1991

Salted brush regime

$$F \simeq \frac{3LkT}{Na^2} + \omega NkT \frac{N\sigma}{L^2} \longrightarrow L_0 \simeq \alpha^{2/3} a^{2/3} N\sigma^{1/3} c_s^{-1/3}$$

L = equilibrium brush height, N = number of monomer units of Kuhn length a, σ = adsorption density, kT = thermal energy, α = ratio of the total number of free mobile counter ions to the total number of monomer segments

Brushes in varying proportions of multi-valent salt $Ru(NH_3)_6^{3+}$ at constant overall ionic strength

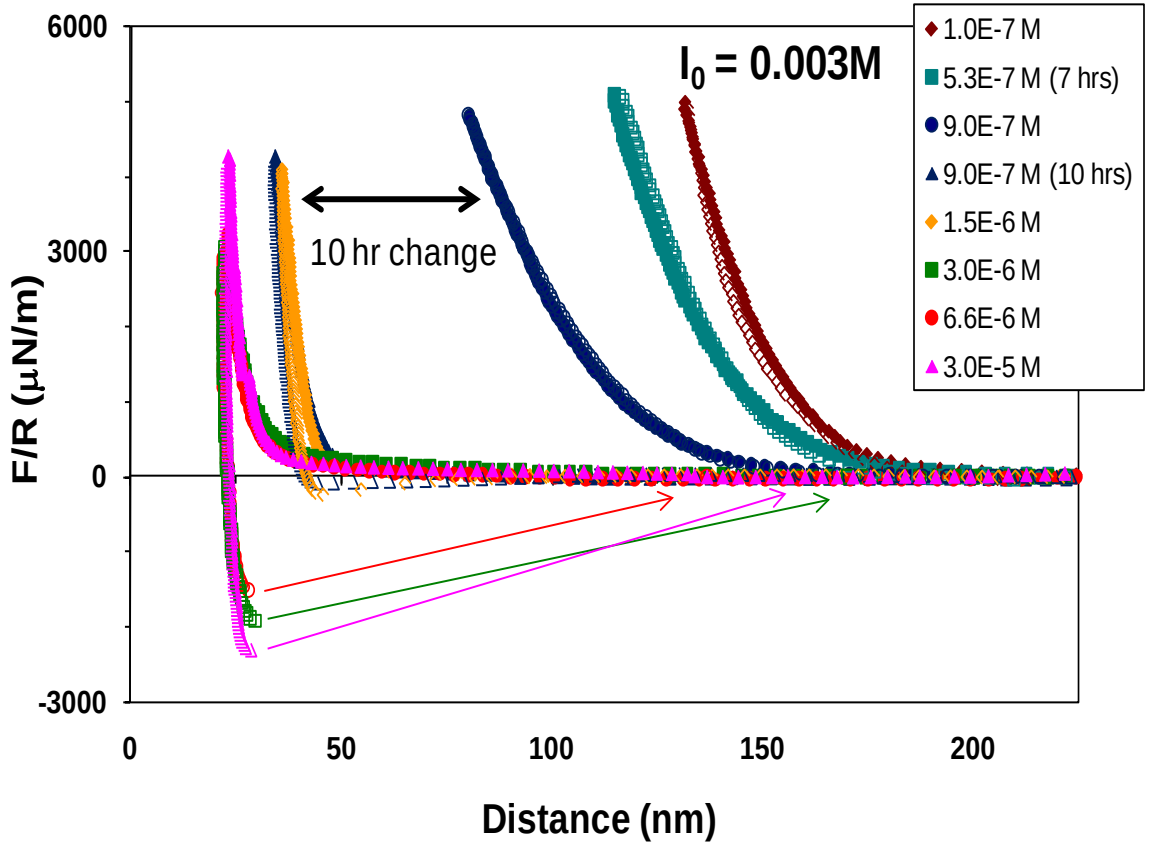

Compression and separation force profiles of $PtBS_{20}$-$NaPSS_{420}$ measured at I_0 = 0.003M. Solid data points represent the compression of the surfaces. Open data points represent separation. Concentrations of $Ru(NH_3)_6^{3+}$ are incrementally increased as indicated in the legend.

THE INSTITUTE FOR MOLECULAR ENGINEERING

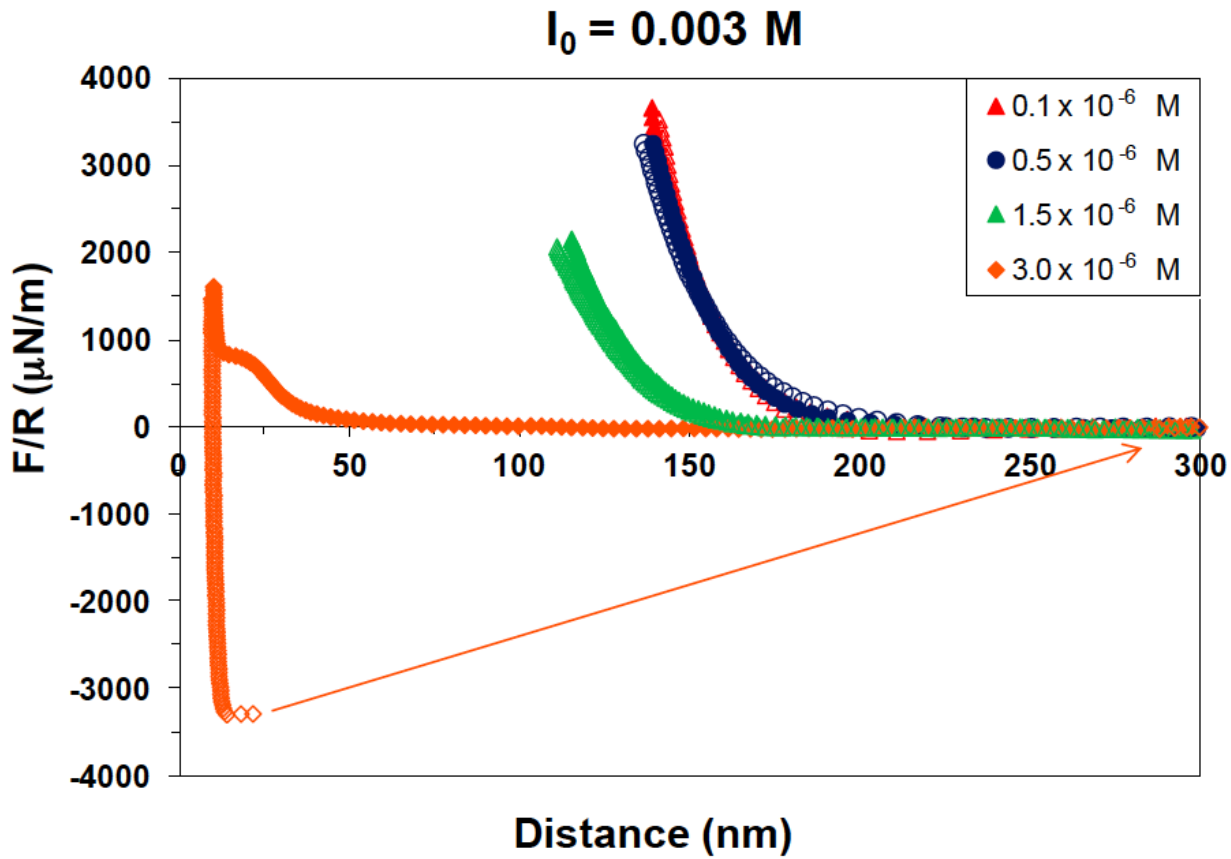

Figure 2: The collapse of two polyelectrolyte brushes and their subsequent adhesion is facilitated by the addition of tri-valent La^{3+} to the bulk solution. Here, the normalized force between two surfaces coated with self-assembled NaPSS brushes (*F/R*) is plotted as a function of distance. This experiment was performed in a fixed overall ionic strength solution of $I_0 = 0.003$ M. Bulk lanthanum concentrations were sequentially increased from the lowest concentration (0.1×10^{-6} M) to the highest (3.0×10^{-6} M), as can been seen in the legend.

Polyelectrolyte Complex Formation

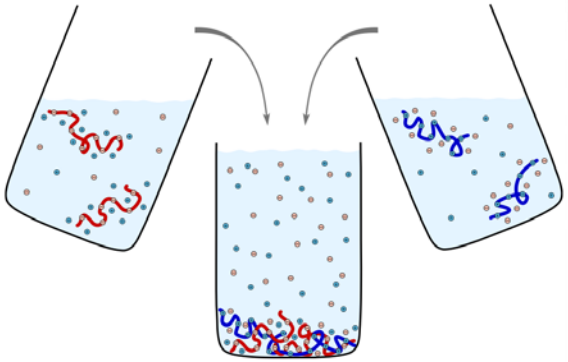

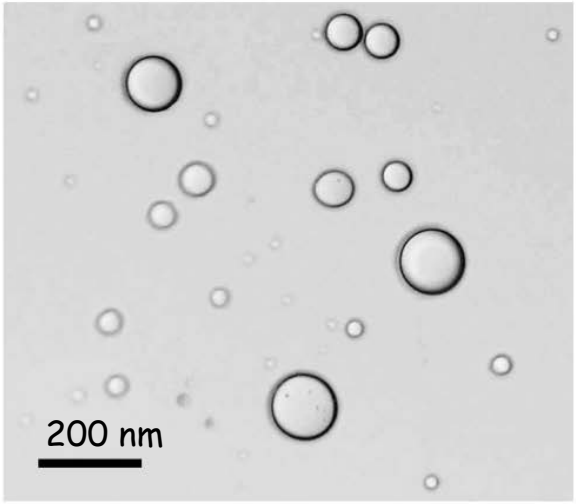

"Interfacial Tension of Polyelectrolyte Complex Coacervate Phases", J. Qin, D. Priftis, R. Farina, S. L. Perry, L. Leon, J. Whitmer, K. Hoffmann, M. Tirrell and J. J. de Pablo, *ACS Macro Letters*, **3**, 565–568 (2014).

"The Effect of Salt on the Complex Coacervation of Vinyl Polyelectrolytes", S. Perry, Y. Li, D. Priftis, L. Leon and M. Tirrell, *Polymers*, **6**, 1756-1772 (2014).

"Complex Coacervation of Poly(ethylene-imine)/Polypeptide Aqueous Solutions: Thermodynamic and Rheological Characterization", D. Priftis, K. Megley, N. Laugel and M. Tirrell, *J. Coll. Interface Sci.*, **398**, 39-50 (2013).

THE INSTITUTE FOR
MOLECULAR
ENGINEERING

Phase Diagram

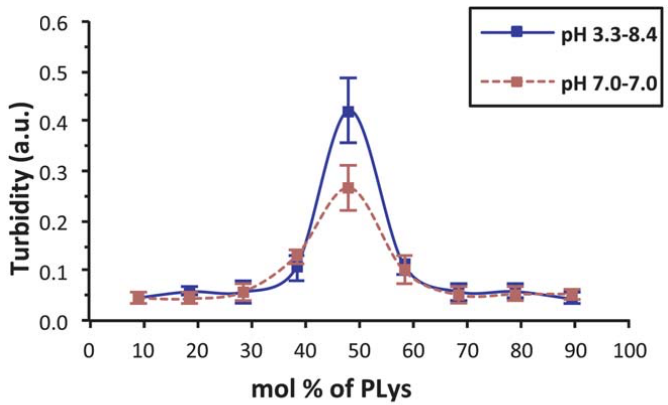

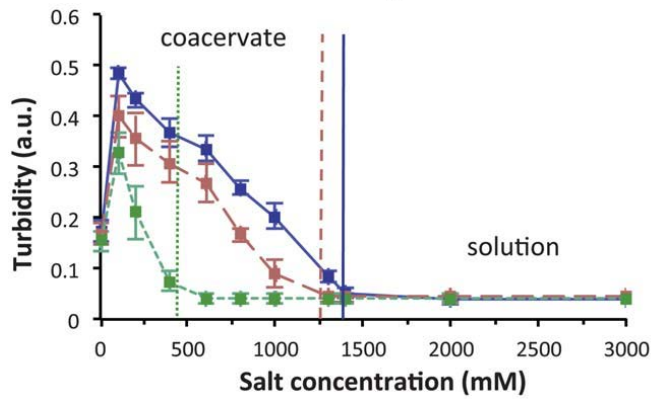

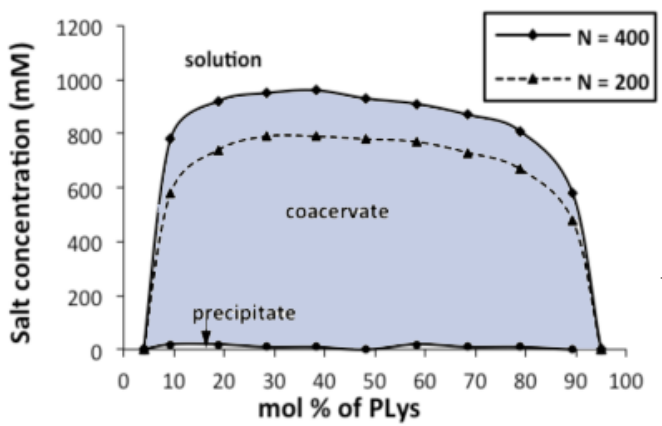

Driving forces

- Electrostatic interactions between the polyelectrolyte chains
- Release of counter ions associated with the polyelectrolyte chains

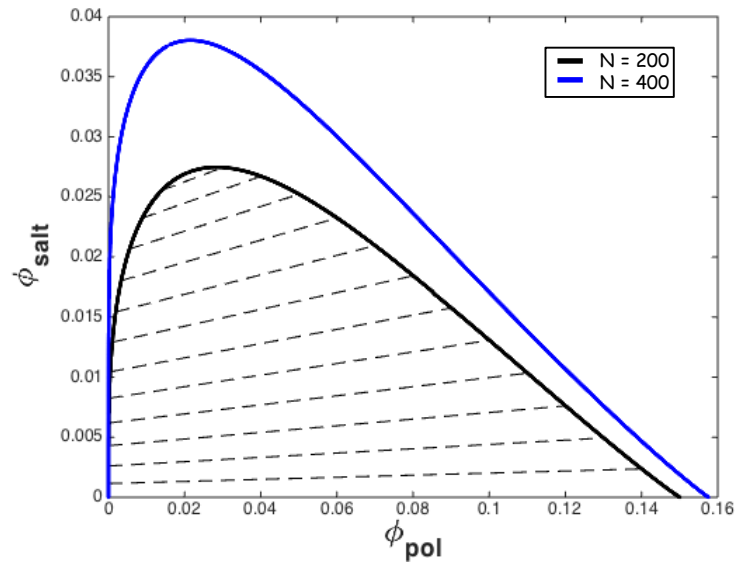

Key Goals

- Predicting PEC properties and stimuli response
- Design of PEC-based self-assembling materials

THE INSTITUTE FOR MOLECULAR ENGINEERING

Figure 6. Plots of turbidity as a function of (**a**) salt concentration and (**b**) ionic strength for a series of chloride salts, investigating the effects of various cations. All samples were prepared at 1 mM total monomer concentration, 50/50 mol% pAA/pAH ratio at pH 6.5. Complexes were prepared by adding pAA to a solution containing a mixture of pAH and the desired quantity of salt.

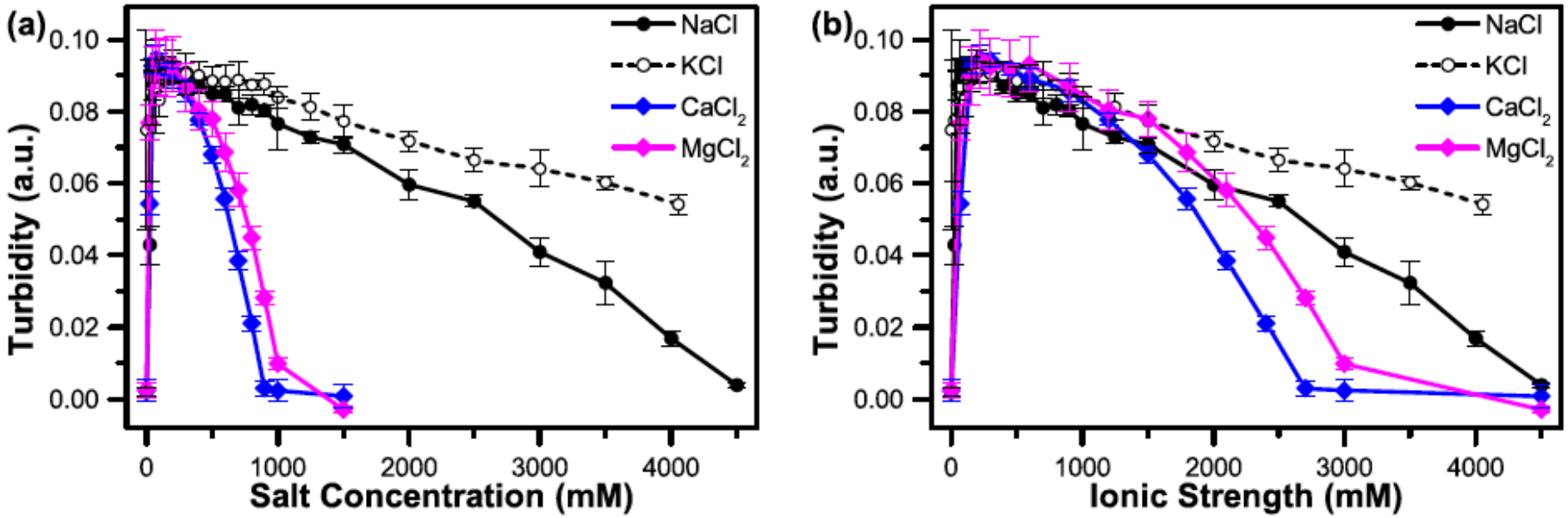

THE INSTITUTE FOR
MOLECULAR
ENGINEERING

Triblock copolymer synthesis:

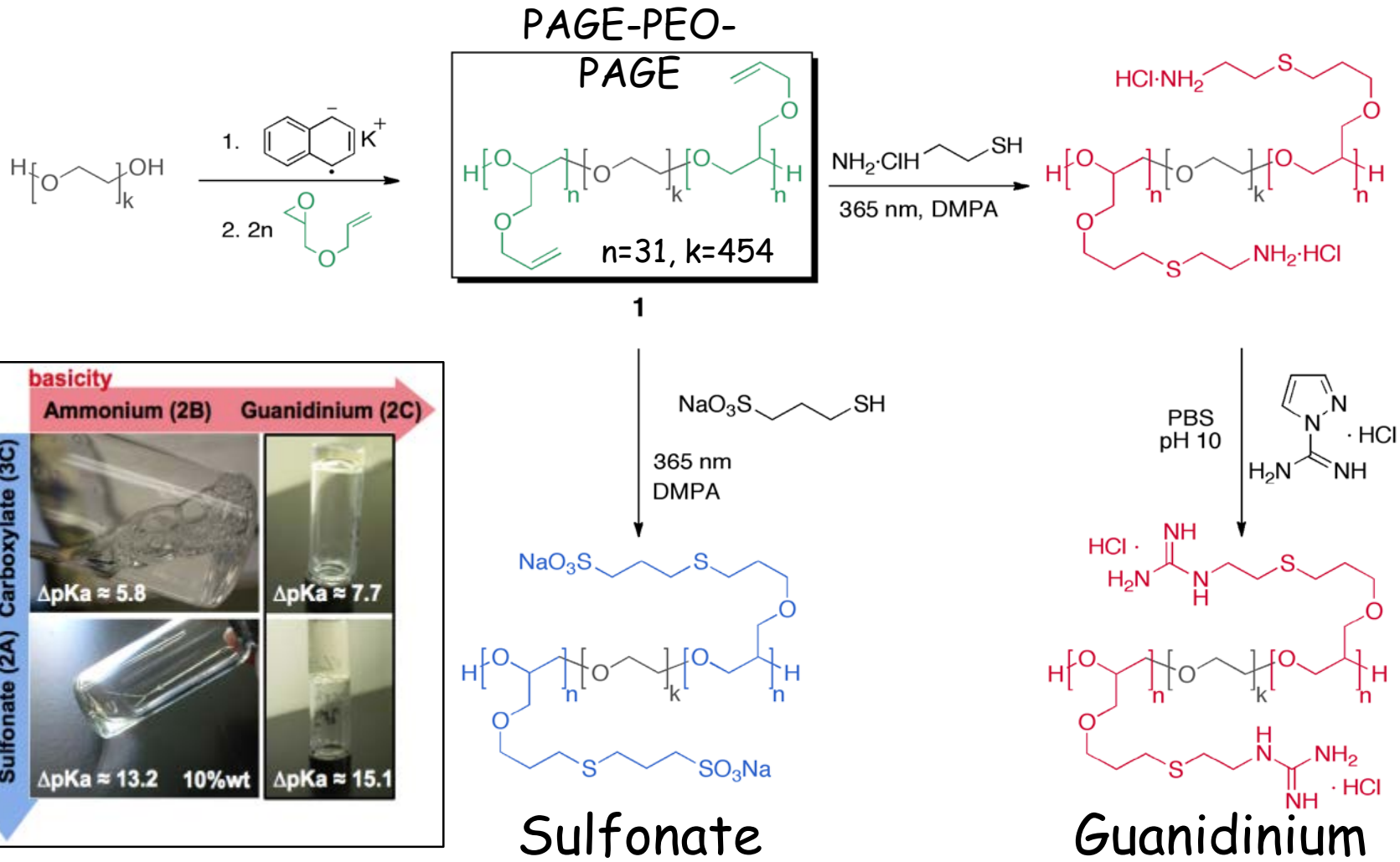

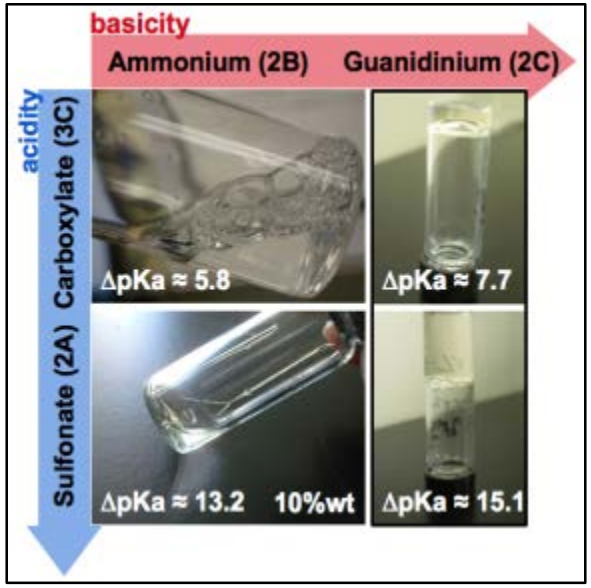

Hunt, JN; Feldman, KE; Lynd, NA; Deek, J; Campos, LM; Spruell, JM; Hernandez, BM; Kramer, EJ; Hawker, CJ; *Adv. Mat.* **2011**

THE INSTITUTE FOR MOLECULAR ENGINEERING

Gels with the BCC structure had the largest G'

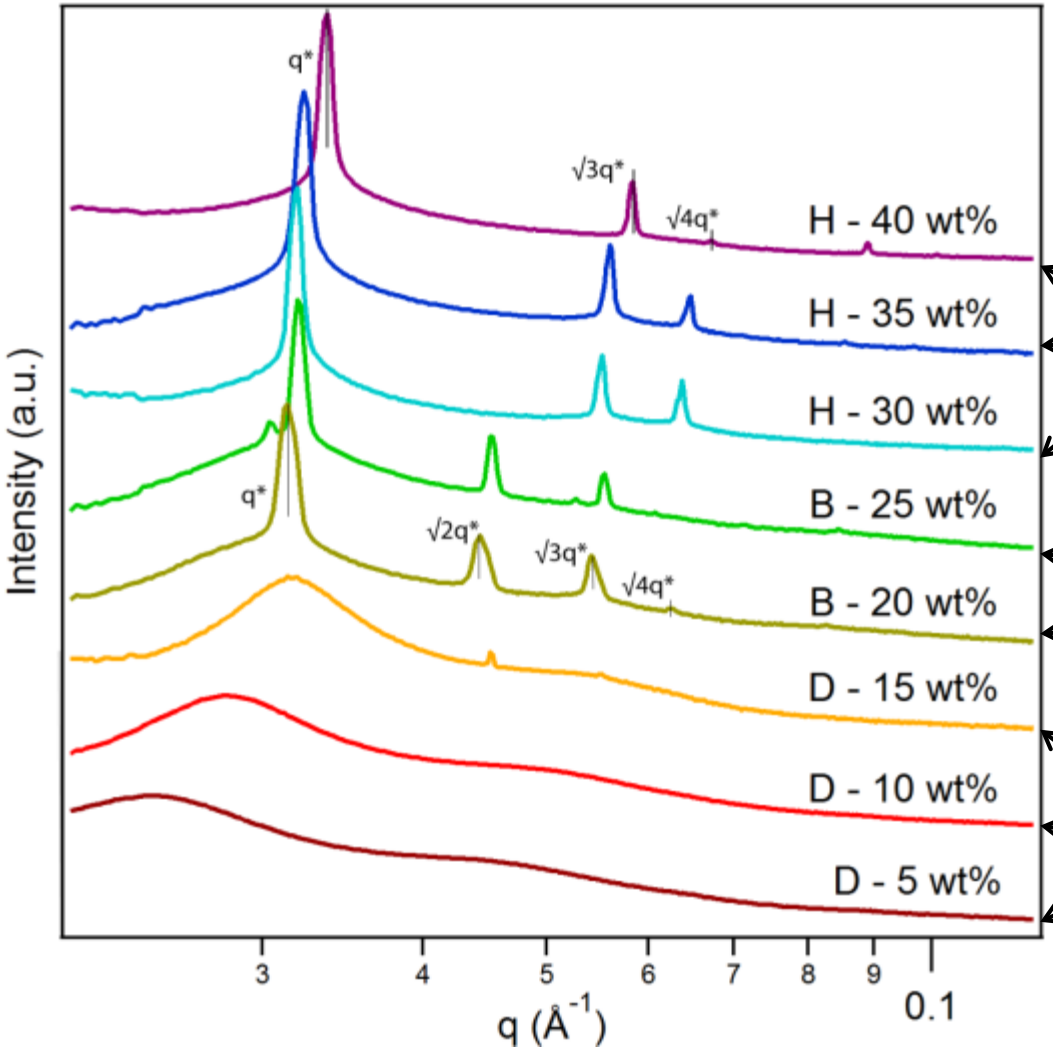

3.5K end blocks. 20K middle blocks
Equimolar mixtures of sulfonate and guandinium polymers

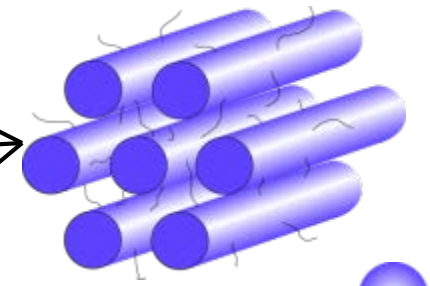

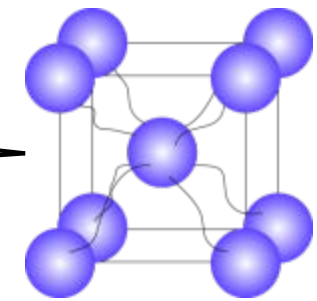

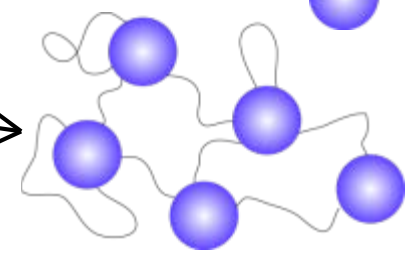

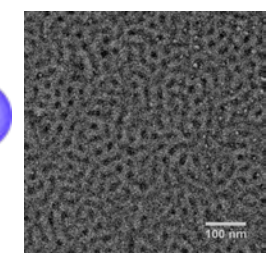

All SAXS data were obtained at the 8-ID-E line at the Advanced Photon Source at Argonne National Laboratory

7.35 keV x-rays, 2.18 m detector distance

D.V. Krogstad, N. A. Lynd, S.-H. Choi, J. M. Spruell, C. Hawker, E. J. Kramer and M. V. Tirrell, *Macromolecules*, 46, 1512-1518 (2013).

THE INSTITUTE FOR MOLECULAR ENGINEERING

Cryo-TEM shows that the domains are fairly monodisperse and well ordered

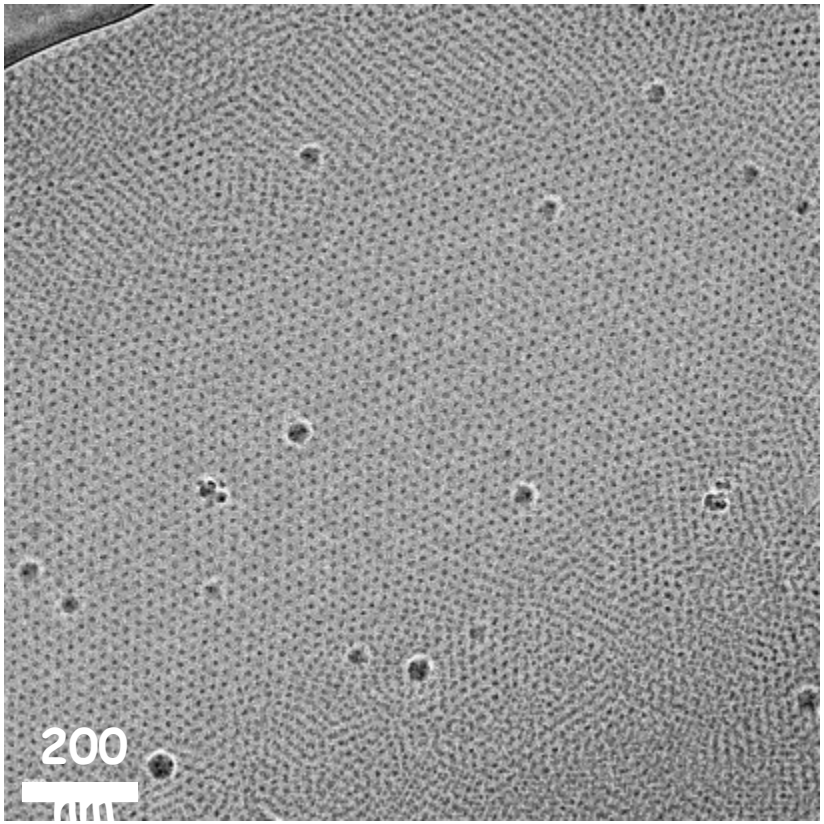

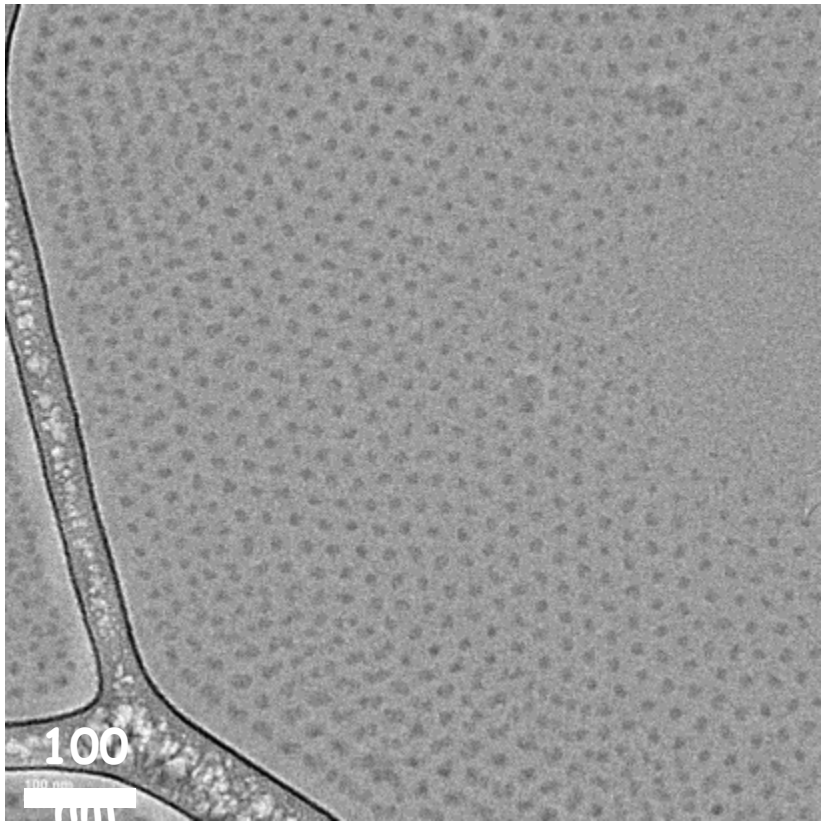

THE INSTITUTE FOR MOLECULAR ENGINEERING

SAXS data show that, as salt is added, the ordered structure of the gels is lost

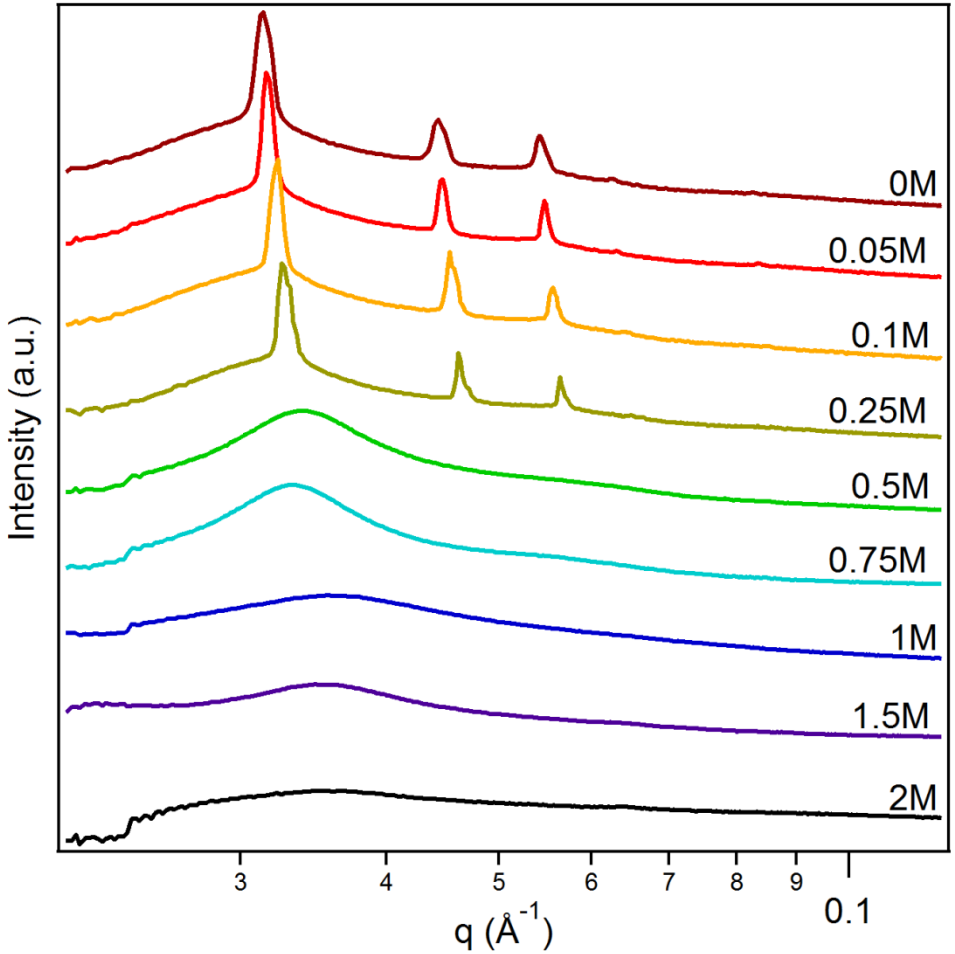

D.V. Krogstad, N. A. Lynd, S.-H. Choi, J. M. Spruell, C. Hawker, E. J. Kramer and M. V. Tirrell, *Macromolecules*, **46**, 1512-1518 (2013).

THE INSTITUTE FOR MOLECULAR ENGINEERING

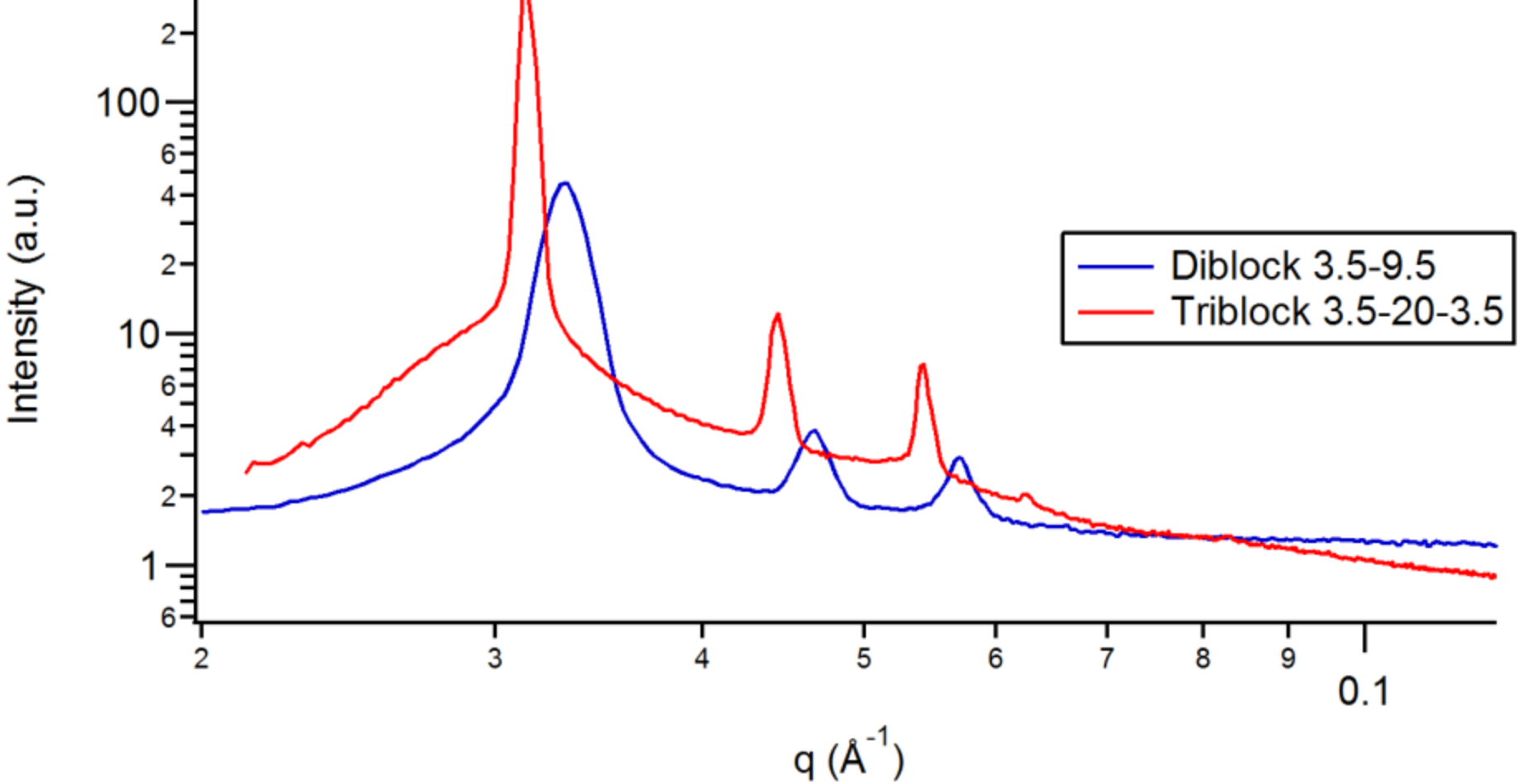

	q at 1st peak (A^{-1})	d spacing (A)	Structure
Triblock	0.0313	200.3	BCC
Diblock	0.0331	189.6	BCC

D.V. Krogstad, N. A. Lynd, S.-H. Choi, J. M. Spruell, C. Hawker, E. J. Kramer and M. V. Tirrell, *Macromolecules*, **46**, 1512-1518 (2013).

THE INSTITUTE FOR MOLECULAR ENGINEERING

The translational correlation lengths increase throughout the experiment

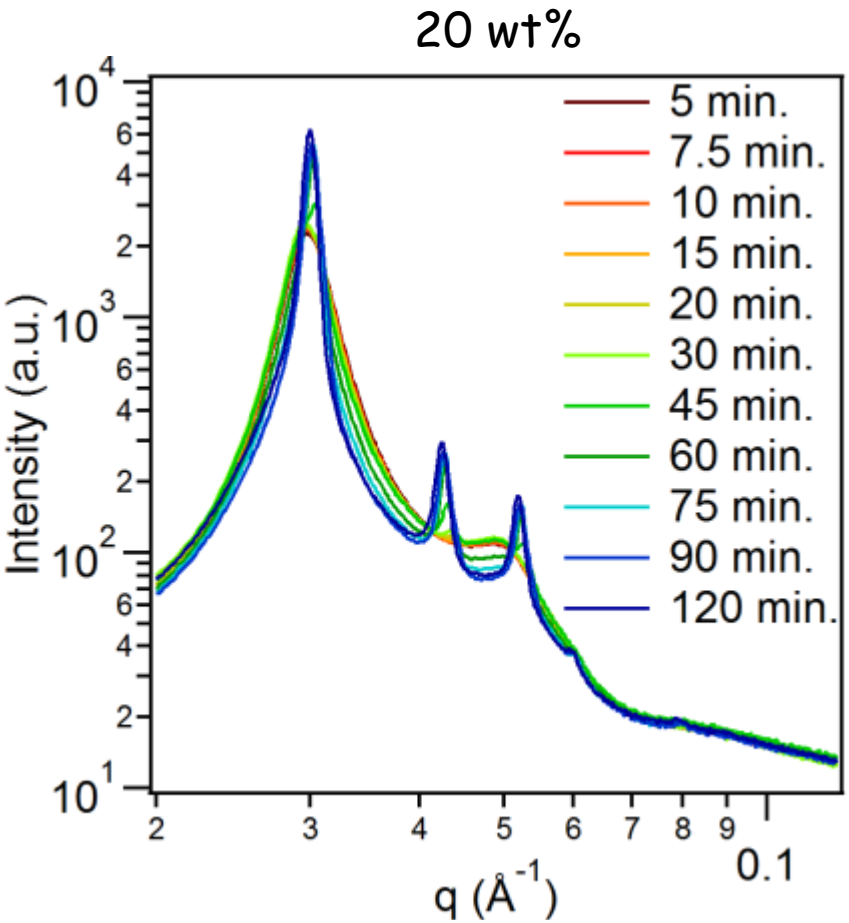

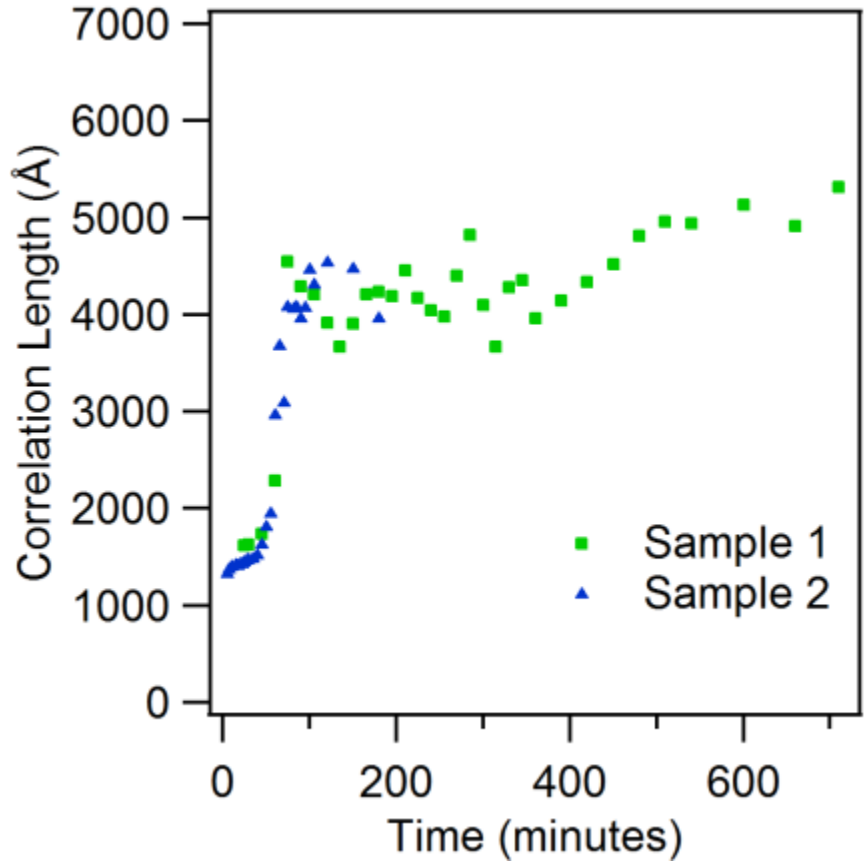

THE INSTITUTE FOR MOLECULAR ENGINEERING

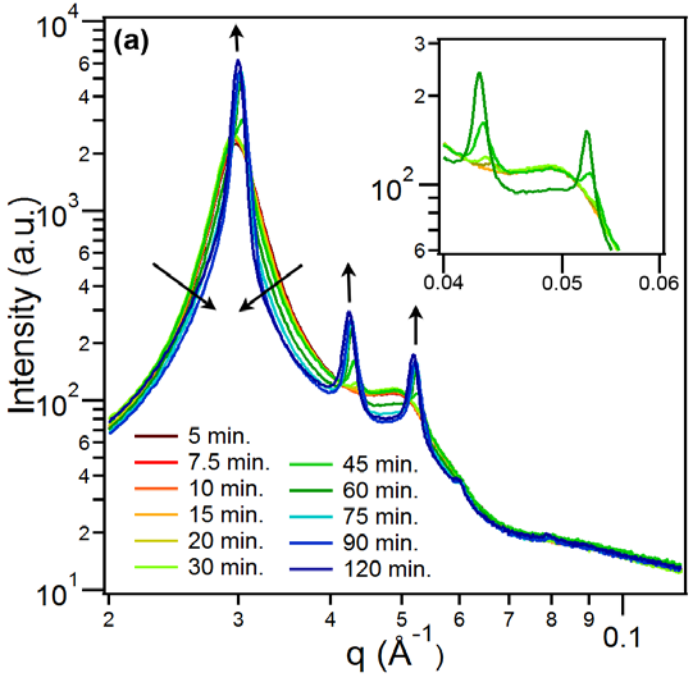

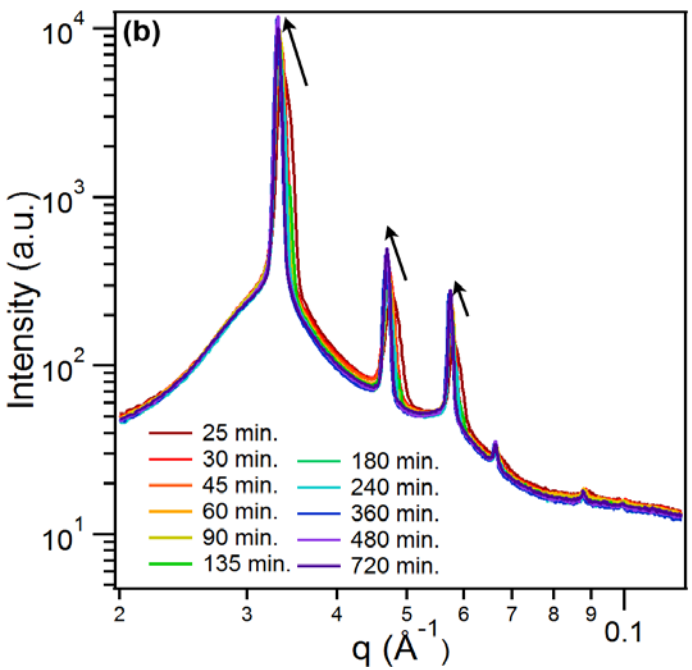

Small angle X-ray scattering was utilized to investigate the structural evolution with time for both the **(a) tri-block and the (b) di-block copolymer materials**. (a) It can be seen that for the tri-block copolymers, the BCC structural peaks were not initially observed, however, starting at about 20-30 minutes, the second and third order BCC peaks started to form. With time, these peaks increased and the width of the first order peak decreased. The formation of the second- and third-order peaks are more clearly visible in the inset showing the 15, 20, 30, 45 and 60 minute patterns. (b) For the di-block copolymers, the BCC structure formed quicker and was observed even at 5 minutes (not shown). Both samples had a polymer concentration of 20 wt% and a salt concentration of 0 M NaCl. The arrows indicate the direction of changes in the SAXS patterns with time.

The structure variation can be summarized schematically in a phase diagram

Triblock Phase Diagram

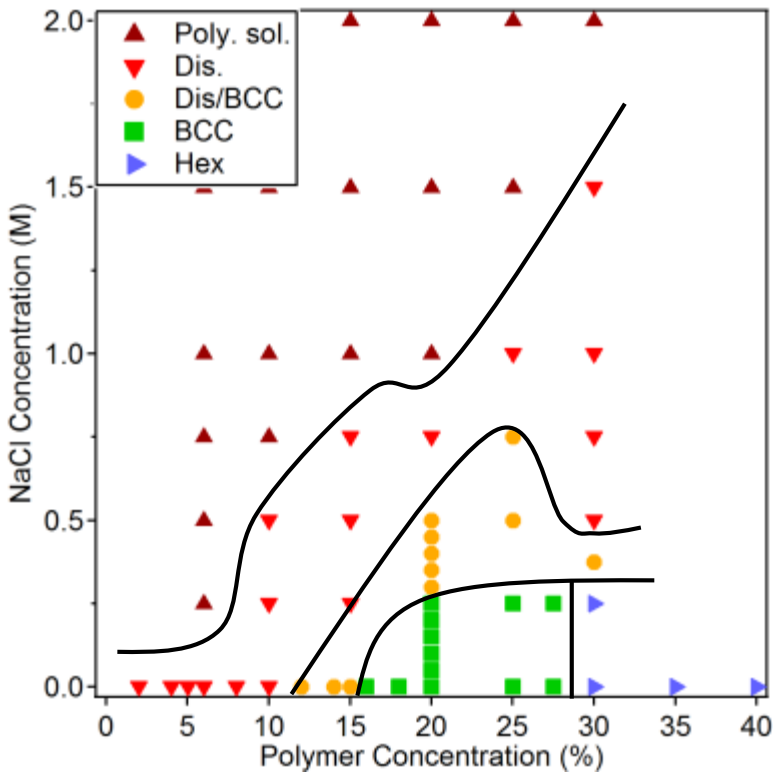

Diblock Phase Diagram

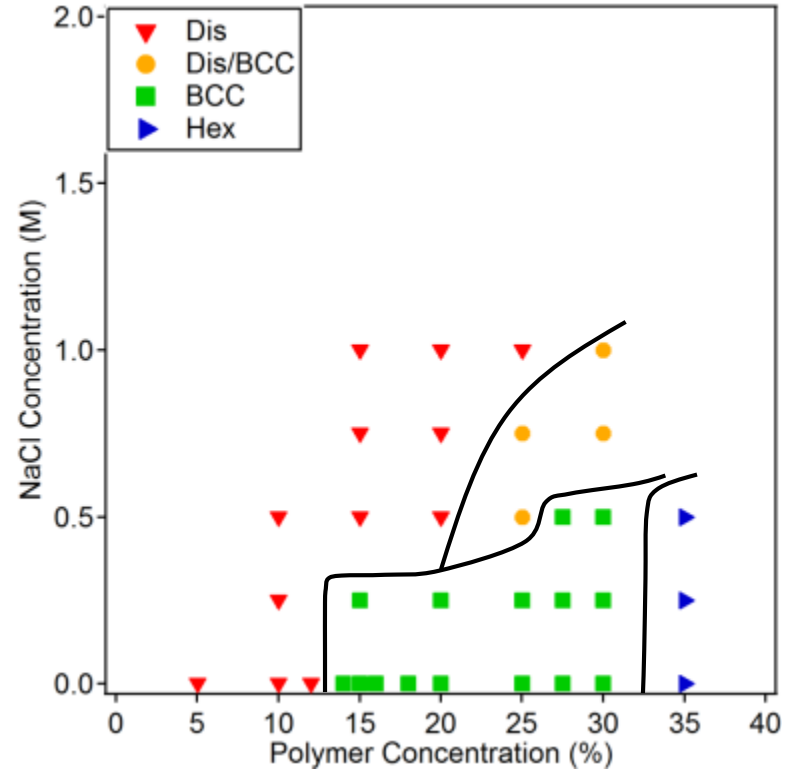

THE INSTITUTE FOR MOLECULAR ENGINEERING

"Structural Evolution of Polyelectrolyte Complex Core Micelles and Ordered-Phase Bulk Materials", D. V. Krogstad, N.A. Lynd, D. Miyajima, J. Gopez, C. J. Hawker, E. J. Kramer, M. Tirrell, *Macromolecules*, **47**, 8026-8032 (2014).

SANS shows changes in the lattice spacing with polymer concentration

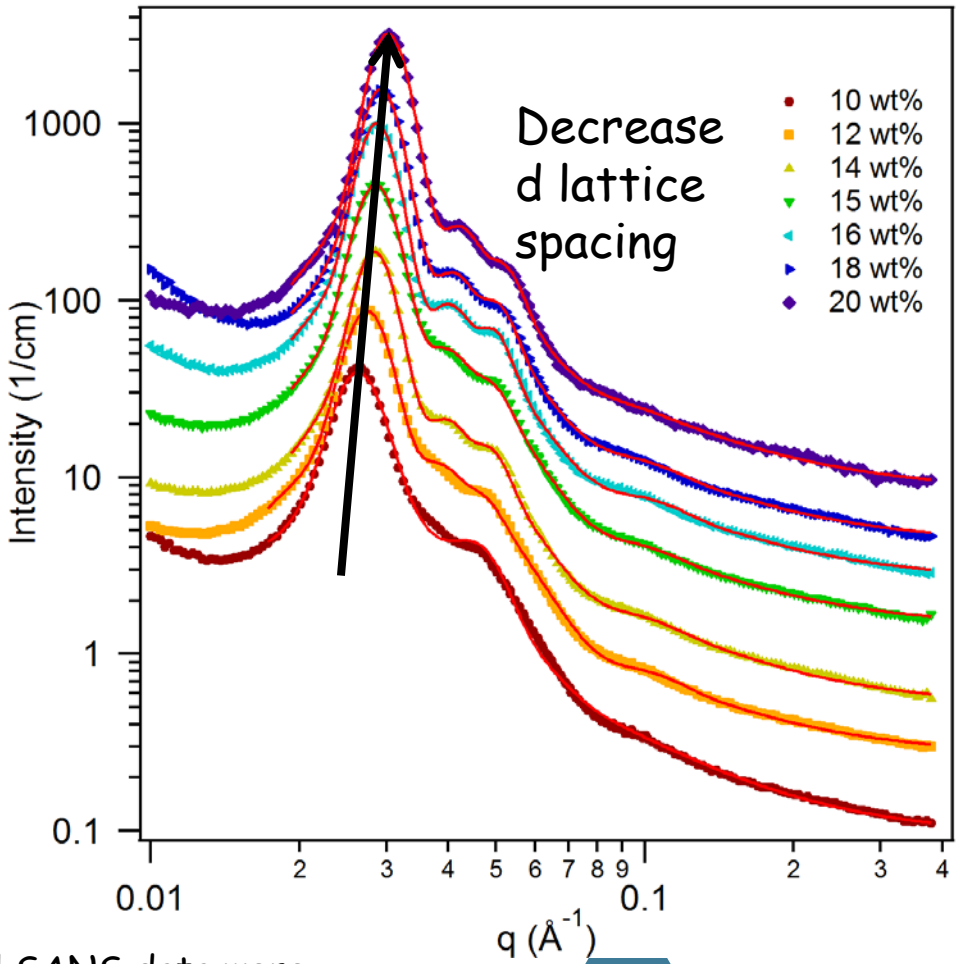

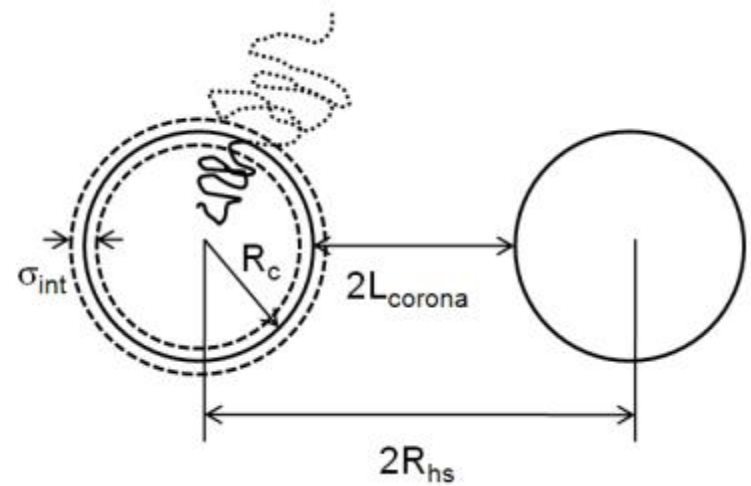

- Core-shell micelles
- Polydisperse core size
- Interfacial thickness between the core and the shell
- Variable hard sphere or BCC structure factor

All SANS data were obtained from the BioSANS-3 line at Oak Ridge National Laboratory

THE INSTITUTE FOR MOLECULAR ENGINEERING

What did we learn from fitting the SANS data?

- Constant domain radius
- Decreased domain spacing
- Decreased water content in the coacervate domains

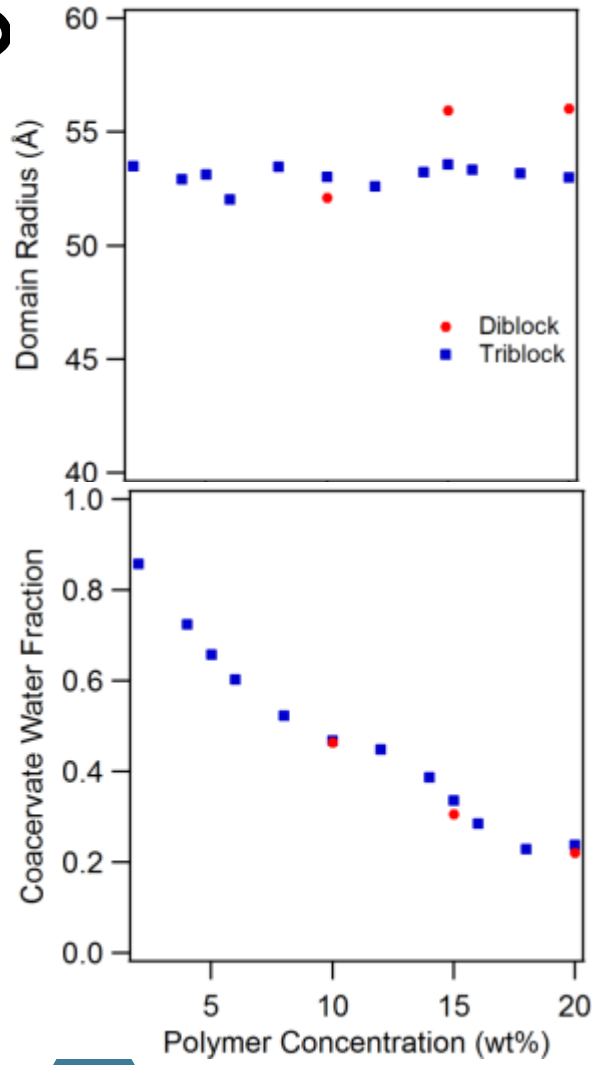

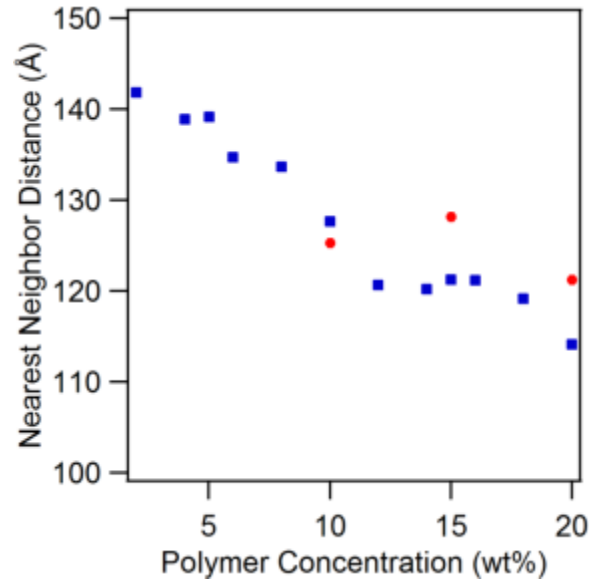

"Small Angle Neutron Scattering Study of Complex Coacervate Micelles and Hydrogels Formed from Ionic Diblock and Triblock Copolymers", D. V. Krogstad, S.-H. Choi, N. A. Lynd, D. J. Audus, S. L. Perry, J. D. Gopez, C. J. Hawker, E. J. Kramer, and M. Tirrell, *Journal of Physical Chemistry B*, 118, 13011–13018 (2014).

THE INSTITUTE FOR MOLECULAR ENGINEERING

Future Trends in Soft Materials with Advanced Light Sources
Journal of Physics: Conference Series **272** (2011) 012004

Sztucki, et al., Scattering from tetradecyltrimethylammonium bromide micelles near the bromine K edge

The total scattered intensity can be decomposed into three components,

$$I(q) = N\{F_0^2(q) + 2f'(E)F_0(q)v(q) + [f'^2(E) + f''^2(E)]v^2(q)\} \quad (6)$$

the energy independent normal SAXS $F_0^2(q)$, a cross-term involving the amplitudes of normal SAXS and the resonant scattering of the counterions, and the pure resonant scattering term (self-term) due to counterions $v^2(q)$. The Fourier transform of the self-term $v^2(q)$ can directly yield the spatial distribution $v(r)$ of the resonant atoms [7,9].

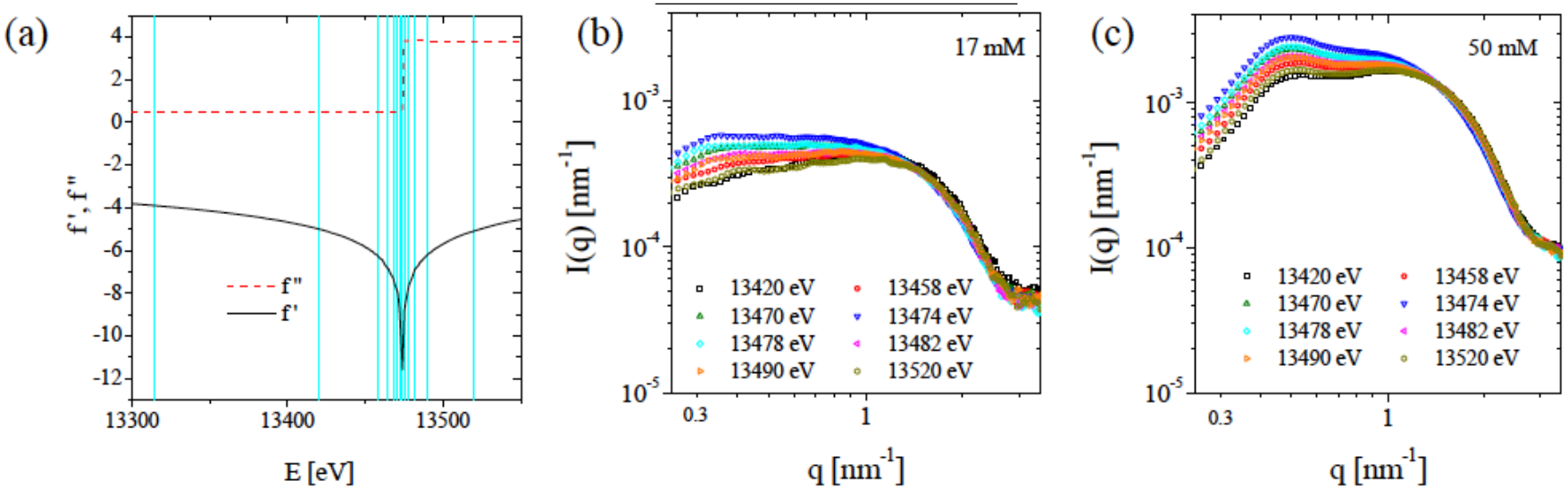

Figure 1. (a) Energy dependent real f' and imaginary f'' parts of the X-ray scattering factor f of bromine near its K-edge (13474eV) depicting the anomalous effect [11]. The vertical lines indicate the energies chosen in this study. (b) and (c) present a selection of the recorded ASAXS data at a sample concentration of 17mM and 50mM, respectively. The fluorescence background was subtracted from all data.

THE INSTITUTE FOR MOLECULAR ENGINEERING

Sztucki, et al., Scattering from tetradecyltrimethyl ammonium bromide micelles near the bromine K edge

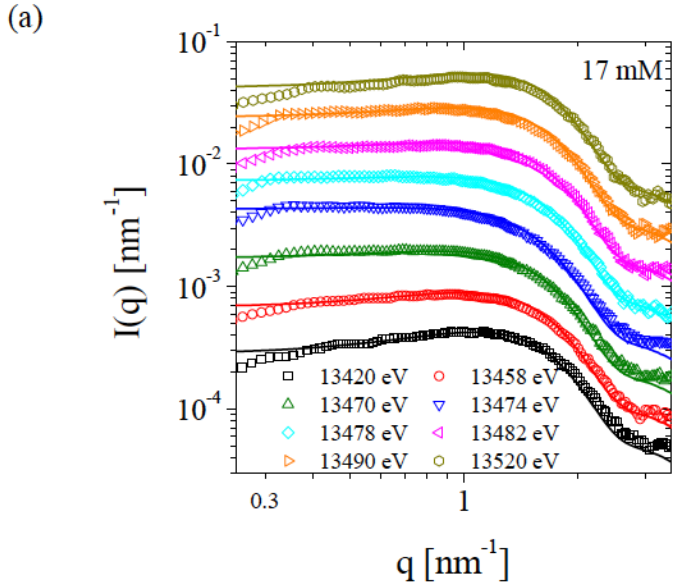

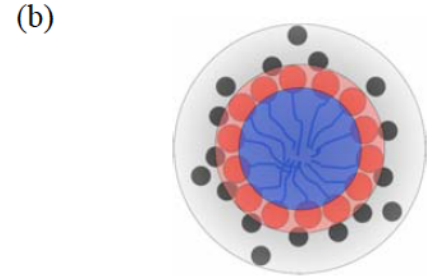

Figure 3. (a) Selected fluorescence corrected datasets (together with their best fits) out of the 14 energies measured in total. All fits were achieved using a unique set of structural parameters. The curves are shifted each by a factor 2 for clarity. (b) Core double shell model used for fitting the ASAXS data simultaneously. See text for more details.

The most interesting fit parameter is the spatial distribution of the bromide ions *v(r)* (black dots) within the outer shell (grey). For data fitting a unique set of structural parameters [*R*, *t*, *v(r)*] was used and only the scattering contrast of the counterion layer [Eq. (5)] was varied according to the effective values of *f'(E)* and *f''(E)*.

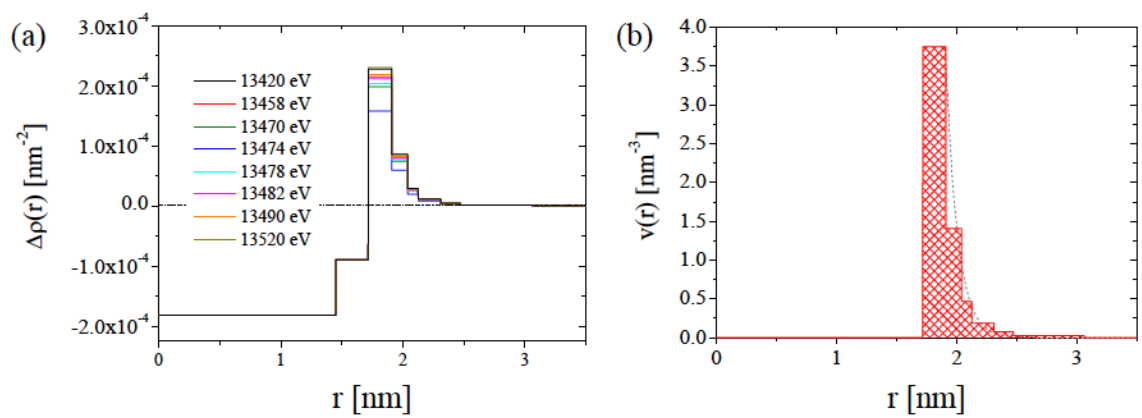

Figure 4. (a) Radial scattering length density profile to the best fits presented in Fig. 3. Only the scattering contrast within the counterion layer changes according to the energy dependence of *f'(E)* and *f''(E)*. (b) Radial distribution of the counterions indicating that they are concentrated in a layer of ~0.34nm thickness with an exponential decay of the histogram to zero at a distance of 3.1nm from the center of the core.

Journal of
Applied
Crystallography

ISSN 0021-8898

J. Appl. Cryst. (2013). **46**, 1407–1413

Received 12 March 2013
Accepted 9 August 2013

Study of the internal structure of polymer micelles by anomalous small-angle X-ray scattering at two edges[1]

doi:10.1107/S0021889813022450

Megumi Sakou,[a] Atsuro Takechi,[a] Shin-ichi Murakami,[a] Kazuo Sakurai[a,b] and Isamu Akiba[a,b]*

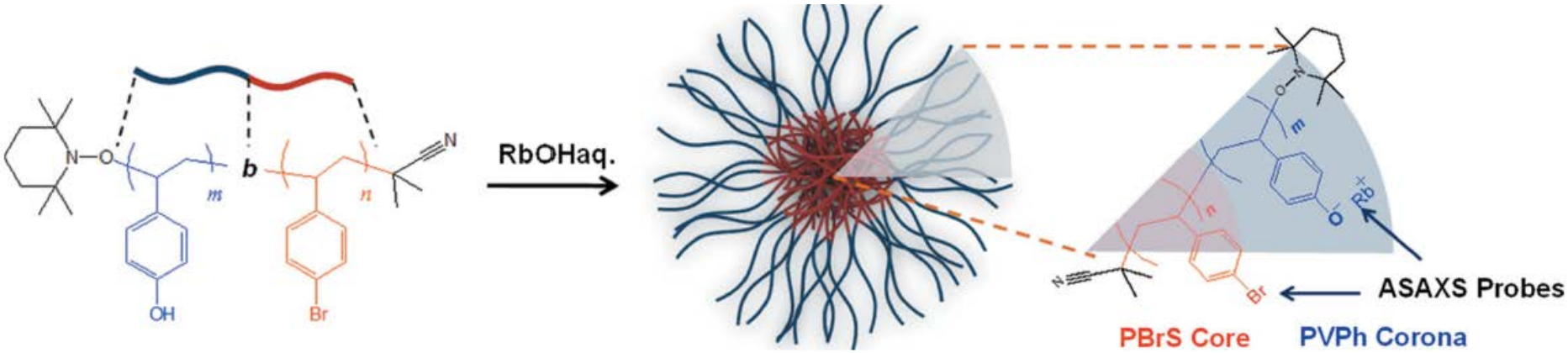

Figure 1
Chemical structure of PVPh-*b*-PBrS and schematic representation of the structure of an RbPVPh-*b*-PBrS micelle.

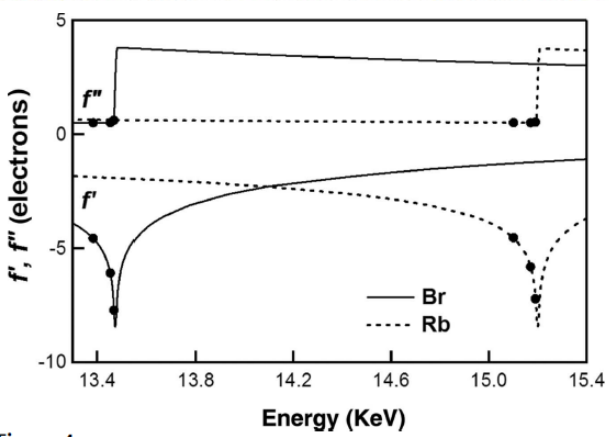

Figure 4
Energy dependence of anomalous scattering factors f' and f'' of Br and Rb. The obtained K edges of Br and Rb were 13.483 and 15.200 keV, respectively. Filled circles indicate the energy of the incident X-ray beam used for ASAXS measurements.

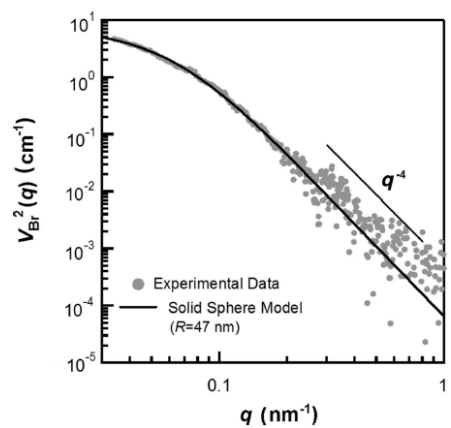

Figure 6
The resonant term obtained from the energy dependence of the SAXS intensity of RbPVPh-*b*-PBrS micelles near the Br K edge. The solid line represents the theoretical curve calculated for a solid sphere.

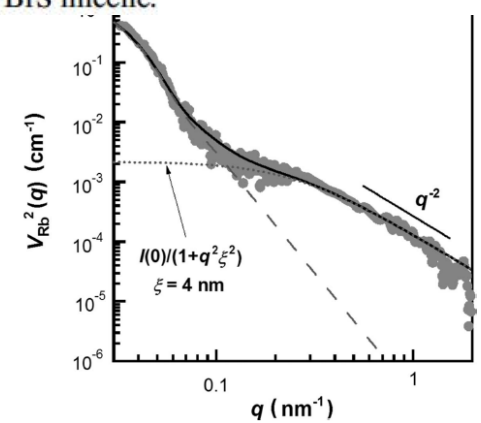

Figure 7
The resonant term obtained from the energy dependence of the SAXS intensity of RbPVPh-*b*-PBrS micelles near the Rb K edge. The dashed line shows the theoretical curve calculated for the particle with the radial concentration distribution shown in Fig. 7. The dotted line is calculated using equation (13). The solid line was obtained by adding the dashed and dotted lines.

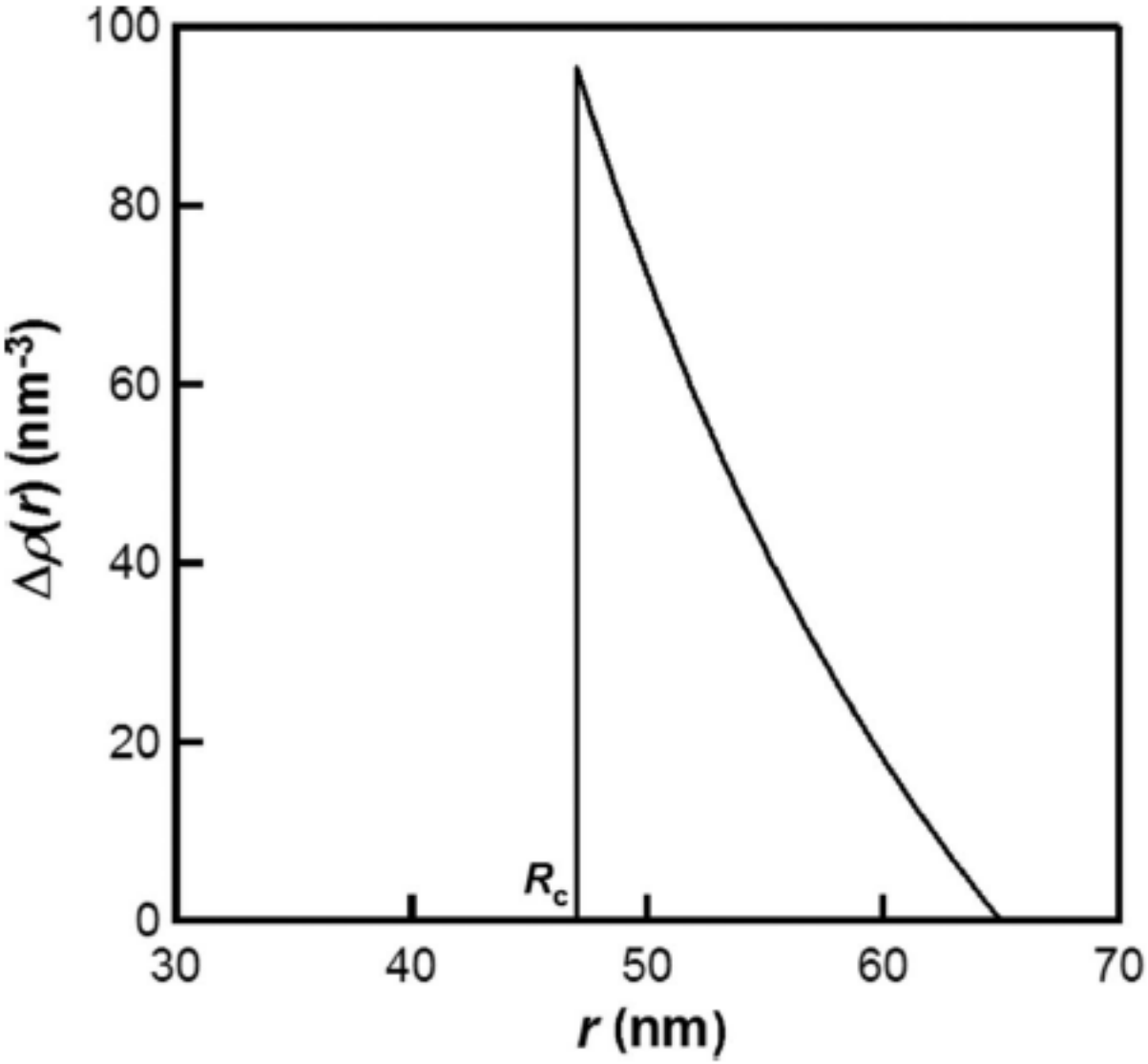

Figure 8
Schematic representation of the radial distribution of Rb^+ in the corona of an RbPVPh-*b*-PBrS micelle.

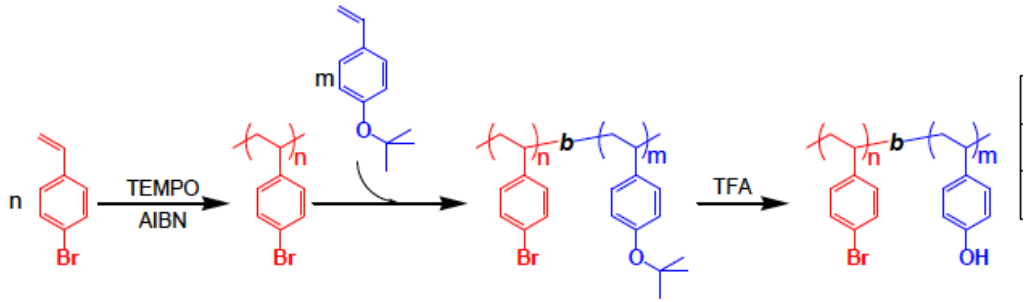

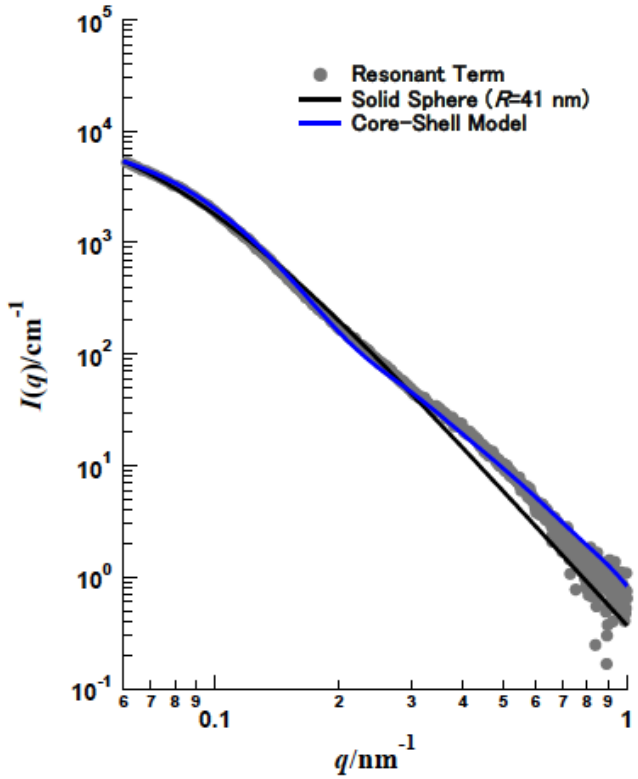

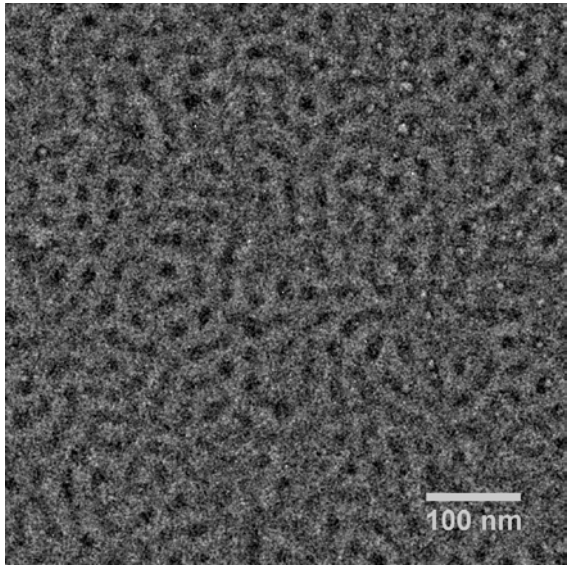

Figure 4. Resonant term obtained from ASAXS measurement for PVPh-*b*-PBrS in TMEDA (ash), and SAXS profiles calculated for hard sphere with 41 nm radius (Black). and Core-Shell model with same radius (Blue).

Ions at Soft Matter Interfaces

Anomalous X-Ray Reflectivity Characterization of Ion Distribution at Biomimetic Membran

David Vaknin,[1] Peter Krüger,[2] and Mathias Lösche[2,3]

[1]*Ames Laboratory and Department of Physics and Astronomy, Iowa State University, Ames, Iowa 50011*
[2]*Institute of Experimental Physics I, Leipzig University, Linnéstrasse 5, D-04103 Leipzig, Germany*
[3]*Department of Chemical and Biomolecular Engineering, The Johns Hopkins University, Baltimore, Maryland 21218, USA*
(Received 2 July 2002; published 1 May 2003)

Anomalous x-ray reflectivity measurements provides detailed information on ion binding to biomembrane surfaces. Using a monochromatic beam tuned to various x-ray energies at the Argonne National Laboratory Advanced Photon Source and utilizing a newly commissioned x-ray liquid surfaces reflectometer, measurements at and away from ion absorption edges allow determination of the distribution of these ions as they accumulate near lipid membranes. As a model, the interaction of Ba^{2+} ions with $DMPA^-$ (1,2-dimyristoyl-*sn*-glycero-3-phosphatidic acid) monolayers at the aqueous surface is studied. We find an unexpectedly large concentration of barium at the interface, ≈ 1.5 per $DMPA^-$, forming a Stern layer of bound ions and a cloud of less densely bound ions near the lipid headgroups. This result can be understood only if one assumes that bound cations are partially speciated, e.g., as $BaOH^+$.

DOI: 10.1103/PhysRevLett.90.178102 PACS numbers: 87.16.Dg, 05.65.+b, 87.14.Cc, 87.64.Bx

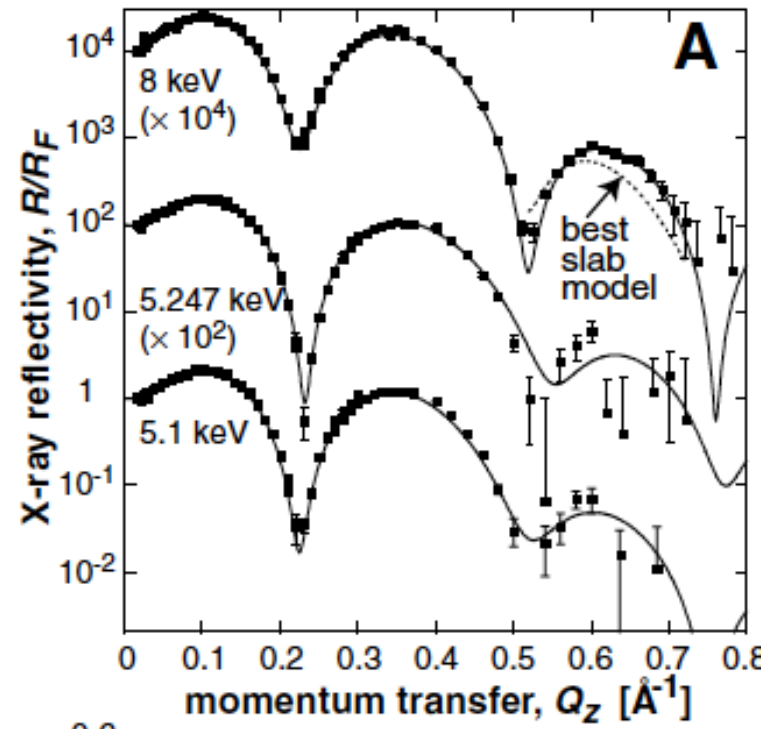

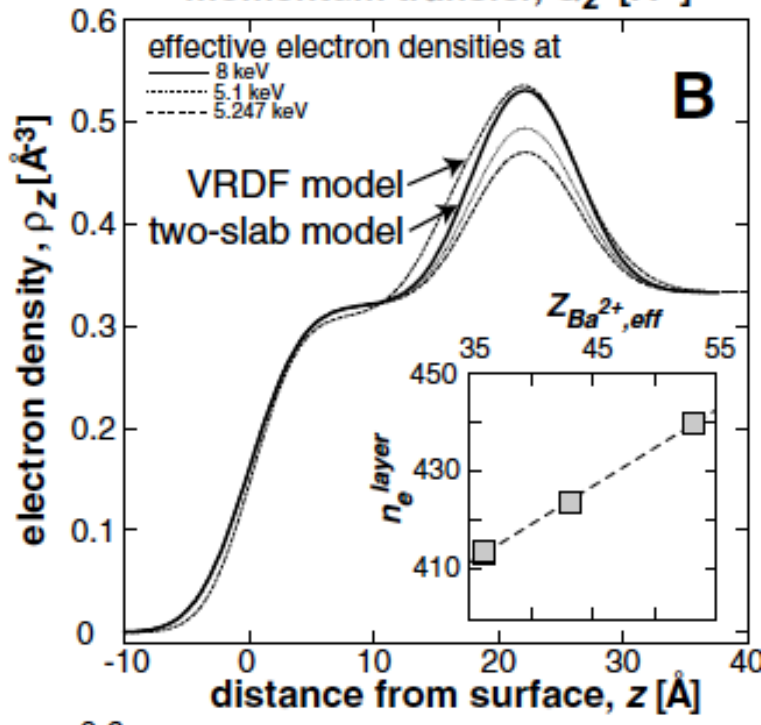

Charged soft matter is fertile territory for high energy x-ray science

THE INSTITU
MOLECU
ENGINEE